Applied Clay Science 46 (2009) 95–101

Contents lists available at ScienceDirect

Applied Clay Science

journal homepage: www.elsevier.com/locate/clay

Reductive transformation of 2-nitrophenol by Fe(II) species in γ-aluminum oxide suspension

Liang Tao [a,b,d], Fangbai Li [b,*], Chunhua Feng [c], Kewen Sun [a,b,d]

[a] Guangzhou Institute of Geochemistry, Chinese Academy of Sciences, Guangzhou 510640, PR China
[b] Guangdong Key Laboratory of Agricultural Environment Pollution Integrated Control, Guangdong Institute of Eco-Environmental and Soil Sciences, Guangzhou 510650, PR China
[c] School of Chemistry and Chemical Engineering, South China University of Technology, Guangzhou 510640, PR China
[d] Graduate School of The Chinese Academy of Sciences, Beijing, 100039, PR China

ARTICLE INFO

Article history:
Received 28 October 2008
Received in revised form 6 July 2009
Accepted 8 July 2009
Available online 17 July 2009

Keywords:
γ-Aluminum oxide
2-Nitrophenol
Fe(II) adsorption
Cyclic voltammetry
Fe(III)/Fe(II) redox potential

ABSTRACT

Fe(II) adsorption onto γ-Al_2O_3 surfaces was studied in view of its high reactivity towards the aqueous reductive transformation of 2-NP. Kinetic measurements demonstrated that rates of 2-NP reduction were highly sensitive to pH, Fe(II) concentration and reaction temperature. An increase in pH, Fe(II) concentration or reaction temperature gave rise to an elevated density of Fe(II) adsorbed to mineral surfaces, which further resulted in an enhanced reaction rate of 2-NP reduction. By using the diffuse double layer (DDL) surface complexation model, the dominant Fe(II) surface complex that was responsible for the high reactivity was predicted to be the strongly bound ≡$SOFe^+$ functional group (represented by ≡$Al_{st}OFe^+$) onto γ-Al_2O_3 surfaces. In addition, cyclic voltammetry tests showed that the enhanced activity of Fe(II) species was attributed to the negative shift of the redox potential of Fe(III)/Fe(II) couple, resulted from the enhanced concentration of ≡$Al_{st}OFe^+$ complex.

1. Introduction

The contamination of soil by nitroaromatic compounds (NACs), one of the ubiquitous pollutants in subsurface environments, is a significant environmental concern (Colon et al., 2006). Recently, an increasing number of laboratory and field studies (Rene et al., 1990; Frank et al., 1992; Rugge et al., 1998; Yan and Bailey, 2001; Naka et al., 2006) have reported that mineral-bound Fe(II) species can substantially promote the reduction transformation of nitro groups to the corresponding anilines under abiotic conditions (Stumm and Sulzberger, 1992; Klausen et al., 1995; Klupinski et al., 2004). Mechanistic studies with this heterogeneous reaction have demonstrated that the formation of surface complexes is responsible for the enhanced reaction rate (Hofstetter et al., 1999; Pecher et al., 2002; Strathmann and Stone, 2003; Li et al., 2008). Depending on environmental factors such as pH, the concentration of Fe(II) and the type of minerals, different Fe(II) surface complex species could exist, varying in their content (Strathmann and Stone, 2003; Hiemstra and Riemsdijk, 2007). Moreover, the contribution of each individual species to the total reaction rate is different. For example, Nano and Strathmann (2008) reported that the concentration of a hydrolyzed surface complex (e.g., ≡TiOFe(II)OH), other than the concentration of aqueous species or the concentration of unhydrolyzed surface complex, was believed to be the key parameter to influence the reactivity of Fe(II) with NACs.

In nature, various minerals included in iron-contained soils (e.g., ferrihydrite, goethite, hematite, etc.) and iron-free soils (e.g., titania, silica and γ-aluminum oxide) are capable of providing functional sites to stabilize Fe(II) ions (Strathmann and Stone, 2003). Of our great interest is the investigation of alumina (Al_2O_3) used as the sole mineral surface for the adsorption of Fe(II) ions, due to the relatively high fraction of alumina in clays, varying from very low to 75% (Schoonen et al., 1998). According to a generalized surface complex model proposed by Strathmann's group, there are two primary surface complexes (weak and strong-binding of ≡$SOFe^+$ functional groups) resulted from the Fe(II) adsorption to γ-AlOOH or γ-Al_2O_3 mineral surfaces (Nano and Strathmann, 2006). The identification of one kind of surface complexes that could play a dominant role in determining the overall reaction activity of NAC transformation is environmentally important, as the concentration of each surface complex is closely correlative with a number of environmental variables. Accordingly, the establishment of such relationships between the reaction rate and the density of dominant surface complex could help to understand the influence of environmental conditions on the reduction transformation of organic pollutants in the presence of Fe(II) and Al_2O_3 minerals.

The interpretation of remarkably enhanced reduction of organic pollutants in a heterogeneous reaction has normally been based on the change of Fe(III)/Fe(II) redox potential in the literature (Klausen et al., 1995). As an example, the Fe oxide mineral surface-bound Fe(III)/Fe(II) couple possesses a more negative redox potential compared

* Corresponding author.
E-mail address: cefbli@soil.gd.cn (F. Li).

0169-1317/$ – see front matter © 2009 Elsevier B.V. All rights reserved.
doi:10.1016/j.clay.2009.07.005

with the aqueous Fe(III)/Fe(II) couple, thus leading to a higher reaction rate (Rush and Koppenol, 1987; Klausen et al., 1995; Buerge and Hug, 1998; Strathmann and Stone, 2002a,b). However, to our knowledge, in spite of the theoretical calculations, no experimental evidence of the difference in redox potential has been available in the previous reports. In fact, the electrochemical method (i.e., cyclic voltammetry (CV)) is a useful tool that enables a direct observation of the redox behavior of the investigated couple, provided that a modified electrode can be successfully produced with minerals.

In this paper, we selected 2-nitrophenol as the target organic contaminant. Experiments were carried out in sterile batch suspensions containing 2-nitrophenol and γ-Al_2O_3 powders under various experimental conditions. The major goal of this study was to explore the interfacial reactions between Fe(II) adsorption and the reductive transformation of 2-nitrophenol. The MINEQL+ (Environmental Research Software) program was applied to calculate the individual equilibrium Fe(II) species in γ-Al_2O_3 suspensions and CV measurements were performed to identify the redox behavior of the adsorbed Fe(II) surface complex.

2. Materials and methods

2.1. Reagents

The γ-Al_2O_3 powders (Shanghai Chemical Reagent Factory (China)) were ground and sifted through 200-mesh before being used. Chemicals including 3-[N-morpholino]propanesulfonic acid (MOPS, >99.5%) and 2-[N-morpholino]ethanesulfonic acid monohydrate (MES, >99.5%) were purchased from Sigma-Aldrich (Germany). Chemicals including 2-nitrophenol (2-NP, 99.5%), 2-aminophenol (2-AB, 99.5%), $FeSO_4 \cdot 7H_2O$ (>99.5%) and methanol (HPLC) were purchased from Acros (Belgium). All chemicals were of analytical or higher grade and were used without further purification.

2.2. Kinetic studies

To prevent Fe(II) oxidation, all experiments were conducted inside an oxygen-free glovebox (Model Bactron II, Anaerobic Chamber, 200 plate capacity, USA). The glovebox atmosphere (99.999% N_2) was continuously bubbled through NaOH solution (1 M) to remove dissolved CO_2. Stock solutions of NaCl (0.20 M), MES (0.05 M), and MOPS (0.05 M) were prepared with reagent-grade water (18 MΩ cm resistivity, Milli-Q water). Stock solution of 2-NP (1.1 mM) was dissolved in methanol in the oxygen-free glovebox, and preserved in a dark-brown container. All solutions were filtered through 0.2 mm filters prior to use. To study the reductive transformation of 2-NP in the presence of γ-Al_2O_3, borosilicate glass serum bottles (20 mL) with aluminum crimps and Teflon-lined butyl rubber septa were employed as reactors. After adding 0.022 mM 2-NP, 3.0 mM $FeSO_4$, 28 mM buffer, and 0.20 M NaCl together with 68.0 mg of γ-Al_2O_3 powders to these reactors, the reduction reactions were started by transferring the serum bottles to an orbital shaker at 200 rpm and 25 ± 1 °C in the dark. Furthermore, to investigate the influences of various factors on the reaction rates, kinetic measurements were carried out over a wide range of conditions (pH from 5.5 to 7.3, Fe(II) concentration in the range between 1.0 mM and 10.0 mM, temperature from 288 K to 318 K). Due to the high possibility of Fe(II) being oxidized at circumneutral pH, the kinetic experiments at pH ≥ 6.5 were conducted with continuously bubbled nitrogen rather than on a rotator. The flow rate of nitrogen was 90 mL min^{-1} which allows for the sufficient stirring of the suspension.

2.3. Adsorption studies

The adsorption of Fe(II) onto γ-Al_2O_3 was conducted under the conditions identical to kinetic experiments, except that 0.022 mM 2-NP was not added to the reactor. Individual batch studies were used to evaluate the influence of pH, Fe(II) concentration and temperature on the extent of Fe(II) adsorption. In detail, pH was changed from 4 to 8; Fe(II) concentrations were varied in the range between 0.1 mM and 0.5 mM; and temperature was modulated from 288 K to 318 K for this investigation. For equilibrium adsorption experiments, Fe(II) species were mixed with solid γ-Al_2O_3 powders for a desired period of time at the controlled pH and temperature. After equilibrium, the final pH of each suspension was recorded before filtering (0.2 μm membrane filter). The acidified filtrate was then collected for the analysis of the Fe(II) content.

2.4. Electrochemical tests

The preparation of a γ-Al_2O_3-modified glassy carbon (GC) electrode started from a bare GC electrode (diameter: 3 mm). Prior to use, the GC electrode was polished with emery paper, followed with γ-Al_2O_3 powders of 1 and 0.06 μm particle size and was thoroughly rinsed with double-distilled water between two polishing steps. Then it was successively cleaned with acetone and double-distilled water in an ultrasonic bath for 10 min, respectively. To obtain a Al_2O_3 slurry, the γ-Al_2O_3 (0.5 mg) was dispersed in a dilute Nafion solution (0.5 wt.%, 250 μL) in an ultrasonic bath for 15 min. By use of a micro-syringe, aliquots (2 μL) of the above suspension was allowed to coat on the clean GC electrode and dry in the air for 30 min prior to measurements.

Electrochemical measurements were carried out in a conventional three-electrode cell, equipped with a γ-Al_2O_3 modified glassy carbon (GC) electrode as the working electrode, a saturated calomel electrode (SCE, + 0.24 V versus the standard hydrogen electrode (SHE) at 25 °C) as the reference electrode, and a platinum spiral wire as the counter electrode. Cyclic voltammograms (CV) were recorded with an Autolab potentiostat (PGSTAT 30, Eco Chemie, The Netherlands) at the scan rate of 50 mV s^{-1}. The electrochemical cell contained 3.0 mM $FeSO_4$ and 0.20 M NaCl solution buffered with 0.028 M MES or MOPS and the solution pH was adjusted by adding diluted HCl or NaOH solution. Pure nitrogen was bubbled through the electrolyte to remove dissolved oxygen. CV tests were performed under pure nitrogen atmosphere at 25 °C.

2.5. Analytical methods

The concentration of 2-NP as a function of time was monitored by HPLC 2487(5 mm Symmetry-C18, 4.6 mm, 250 mm, Waters, USA), which consists of a Waters 1525 Binary pump, an analytical reversed-phase column and a Waters dual λ Absorbance UV/Vis detector. The isocratic mobile phase contained 80/20 (V/V) of methanol/water and 3 mM of HCl at a flow rate of 1.0 ml min^{-1} under isocratic conditions at 30 ± 1 °C and the wavelength was set at 213 nm. Concentrations of 2-NP were calculated by comparison with standard solutions (Klupinski et al., 2004). For kinetic studies, one of the 20-ml serum bottles was taken from the shaker and transformed to the oxygen-free glovebox prior to routine analysis. After being mixed vigorously, the serum bottle was opened and spiked with 2 M HCl (<60 μL) to give a pH<3, preventing further degradation of 2-NP. The suspension was immediately centrifuged at 10,000 rpm for 10 min (Sigma-3K 15) to remove the particles and the supernates were remained for further analysis.

The remaining Fe(II) concentration was determined by the 1,10-phenanthroline method at 510 nm using a UV–visible spectrophotometer (TU-1800PC, Beijing Purkinje General Instrument Co. Ltd.) (Fadrus and Malý, 1975; Maithreepala and Doong, 2004; Jeon et al., 2005). The surface complexation of Fe(II) to γ-Al_2O_3 surfaces was obtained according to a two-site model that considers the formation of $\equiv SOFe^+$ complexes at both weak-binding and strong-binding sites (Nano and Strathmann, 2006). The MINEQL+ (Environmental Research Software) program was applied to calculate individual

equilibrium Fe(II) species in γ-Al_2O_3 suspensions by use of the thermodynamic data listed in Table 1.

3. Results and discussion

3.1. Reductive transformation of 2-NP by Fe(II) in γ-Al_2O_3 suspension

The reduction of 2-NP in reaction media consisting of Fe(II) and γ-Al_2O_3 was studied at pH 6.7 and a temperature of 298 K. Fig. 1 shows the comparisons of reaction kinetics obtained under different conditions. Apparently, no loss of 2-NP was observed in the suspension absent of Fe(II), indicating the adsorption of 2-NP to γ-Al_2O_3 surfaces can be neglected. In addition, the homogeneous reaction of Fe(II) with 2-NP gave a much lower rate than that resulting from the heterogeneous reaction in which the adsorbed Fe(II) species were involved. These observations demonstrated that Fe(II) adsorbed to γ-Al_2O_3 was a reactive electron acceptor to promote the reductive transformation of 2-NP. Further analysis of the linear relationship between $ln\frac{[2NP]_t}{[2NP]_0}$ and reaction time revealed that the transformation of 2-NP generally follows a first-order kinetic rate law in the system containing Fe(II), 2-NP and γ-Al_2O_3. That is,

$$ln\frac{[2NP]_t}{[2NP]_0} = -kt \quad (1)$$

where $[2NP]_0$ and $[2NP]_t$ (M) are concentrations of 2-NP respectively detected at the initial time and at the reaction time, respectively; k (min^{-1}) is the first-order kinetic constant of 2-NP transformation; and t (min) is the reaction time.

Table 1
Summary of γ-Al_2O_3 properties, experimental conditions, and equilibrium models of aqueous reactions and surface complexation reactions.

	γ-Al_2O_3
Specific surface area ($m^2\ g^{-1}$)	136.5[a]
Mineral loading ($g\ L^{-1}$)	4
Total Fe(II) concentration (mM)	0.1–10
pH range	5.5–7.3
Ionic strength (M)	0.2
Equilibration time (h)	4
Aqueous reactions[b]	log *K*
$H_2O \leftrightarrow OH^- + H^+$	−13.997
$Fe^{2+} + H_2O \leftrightarrow FeOH^+ + H^+$	−9.397
$Fe^{2+} + 2H_2O \leftrightarrow Fe(OH)_2^0 + 2H^+$	−20.494
$Fe^{2+} + 3H_2O \leftrightarrow Fe(OH)_3^- + 3H^+$	−28.991
$Fe^{2+} + 4H_2O \leftrightarrow Fe(OH)_4^{2-} + 4H^+$	−45.988
$Fe^{2+} + Cl^- \leftrightarrow FeCl^+$	−0.200
Surface reactions	log *K*[e]
N_w (sites nm^{-2})[c]	2.3
N_s (sites nm^{-2})[d]	0.079 ± 0.004
Surface acid-base reactions[b]	log *K*
$\equiv SOH + H^+ \leftrightarrow \equiv SOH_2^+$	7.7
$\equiv SOH + H_2O \leftrightarrow \equiv SO^- + 2H^+$	−10.2
Fe(II) sorption reactions	log *K*[f]
$\equiv S_wOH + Fe^{2+} \leftrightarrow \equiv S_wOFe^+ + H^+$	−3.70 ± 0.03
$\equiv S_sOH + Fe^{2+} \leftrightarrow \equiv S_wOFe^+ + H^+$	−0.66 ± 0.03

[a] The specific surface area ($m^2\ g^{-1}$) was measured by the Brunauer–Emmett–Teller (BET) method, in which the N_2 adsorption at 77 K using a Carlo Erba Sorptometer was applied.
[b] Ref.(Martell et al. 1997).
[c] Density of weak-binding surface sites.
[d] Density of strong-binding surface sites.
[e] Ref. (Torrents, 1992).
[f] Ref. (Nano and Strathmann, 2006).

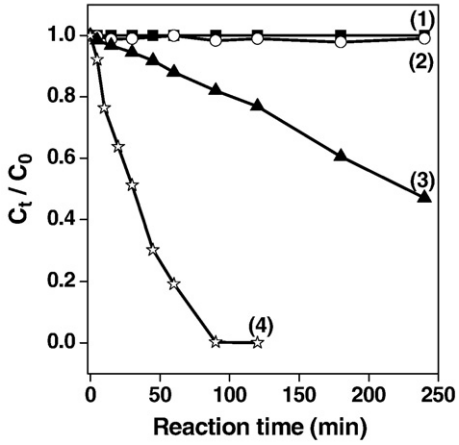

Fig. 1. Reductive transformation of 2-NP at pH 6.7 and 298 K under different conditions, (1) blank reaction; (2) 2-NP and γ-Al_2O_3 powder; (3) 2-NP and $FeSO_4$; and (4) 2-NP, $FeSO_4$ and γ-Al_2O_3 powder. Reaction conditions: 3 mM $FeSO_4$, 0.022 mM 2-nitrophenol, 0.2 M NaCl, 4.0 g L^{-1} γ-Al_2O_3. C_t = concentration of 2-NP at time t; and C_0 = concentration of 2-NP at time zero.

3.2. Effects of pH and Fe(II) concentration on 2-NP transformation

The effect of pH on the reductive transformation of 2-NP by Fe(II) in γ-Al_2O_3 suspensions is presented in Fig. 2A. It can be seen that there is a linear correlation between ln k and pH. The high coefficient of determination obtained ($R^2 = 0.96$) indicated that the reaction rates

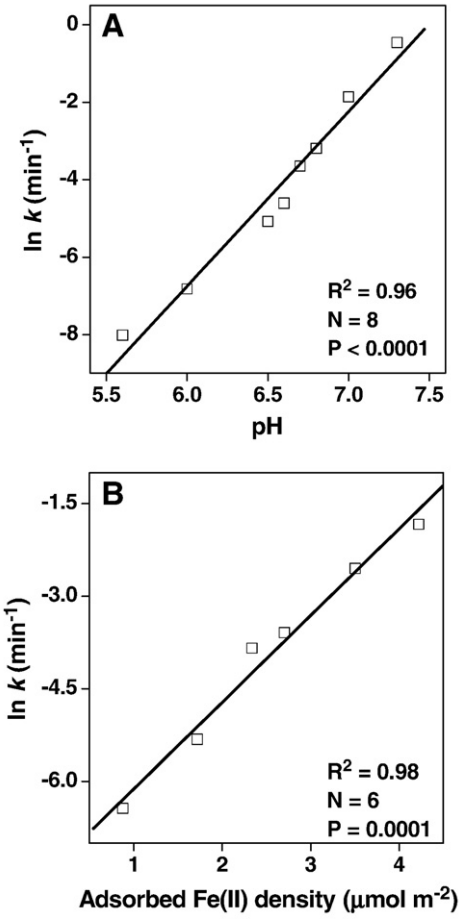

Fig. 2. Effects of (A) pH and (B) adsorbed Fe(II) density on ln k (the first-order rate constant of 2-NP transformation). Reaction conditions: 1–10 mM $FeSO_4$, 0.022 mM 2-nitrophenol, 0.2 M NaCl, 4.0 g L^{-1} γ-Al_2O_3, pH 5.5–7.3, and 298 K. $FeSO_4$ concentration was fixed at 3 mM for (A) experiments and pH was fixed at 6.7 for (B) experiments.

of 2-NP reduction in the presence of Fe(II) and γ-Al_2O_3 were highly sensitive to the change of pH. An increase in pH gave rise to an enhanced reaction rate. The *k* value of 2-NP transformation was found to be 0.0004 min^{-1} at pH 5.5 which was around 100 times smaller than that obtained at pH 6.7. The highest *k* value among all investigated pH was 0.3383 min^{-1} at pH 7.3. This distinctly pH-dependent *k* value was in good accordance with those observed for the reduction of nitroaromatic compounds (NACs) in the appearance of Fe(II) and other mineral suspensions (Colon et al., 2006; Klausen et al., 1995).

Another set of experiments were performed with various Fe(II) concentrations in the range from 1 mM to 10 mM to evaluate its influence on the reduction kinetics of 2-NP transformation at a fixed pH value of 6.7. The change of *k* value was plotted against the density of adsorbed Fe(II) instead of the initial Fe(II) concentration as previous reports have demonstrated that the concentration of adsorbed Fe(II) plays a tremendous role in the NACs reductive transformation (Hofstetter et al., 1999; Li et al., 2008; Pecher et al., 2002; Strathmann and Stone, 2003). The concentration of aqueous Fe (II) indeed had an insignificant effect on the 2-NP transformation as shown in the former section. Fig. 2B reveals the pronounced linear relationship between ln *k* and the density of the adsorbed Fe(II), indicating that the 2-NP transformation was highly dependent on this parameter. For example, the concentration of the adsorbed Fe(II) equalling to 0.8 μmol m^{-2} corresponded to a *k* value of 0.0016 min^{-1}, which was much lower than a *k* value of 0.16 min^{-1} in the presence of 4 μmol m^{-2} adsorbed Fe(II).

3.3. Effects of temperature on 2-NP transformation

The reductive transformation of 2-NP by Fe(II) in γ-Al_2O_3 suspensions also strongly depends on the temperature of the experiment in addition to factors such as pH and Fe(II) concentration. Laboratory batch experiments were performed to quantify the impact of temperature on the 2-NP reduction by varying temperatures in the range from 288 K to 318 K. Fig. 3 shows the corresponding plot of *k* values versus temperature. Clearly, raising temperature was beneficial to the reduction reactions as evidenced from the increase in the *k* value. In comparison to the reaction occurring at 288 K, the rates of the 2-NP transformation by Fe(II) on γ-Al_2O_3 were greatly enhanced at elevated temperatures. The *k* value for the 2-NP transformation increased from 0.0096 min^{-1} to 0.0263 min^{-1}, 0.0623 min^{-1}, and 0.1729 min^{-1} relevant to the investigated temperature changing from

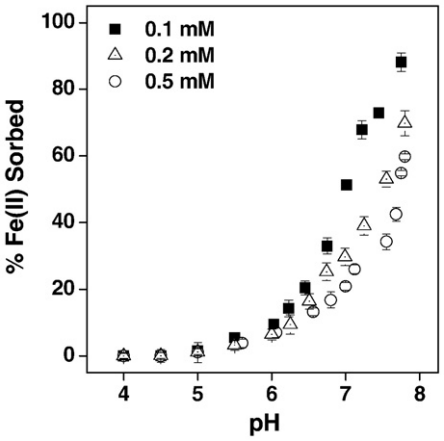

Fig. 4. Effects of pH and Fe(II) concentration on the adsorption of Fe(II) onto γ-Al_2O_3 surfaces. Reaction conditions: 0.1–0.5 mM $FeSO_4$, 0.2 M NaCl, 4.0 g L^{-1} γ-Al_2O_3, pH 4–8, and 298 K.

288 K to 298, 318, and 328 K, respectively. The temperature dependence of the reaction rate can be described by the Arrhenius equation.

$$k = Aexp - \frac{E_a}{RT} \quad (2)$$

Where *A* is the frequency factor, E_a is the activation energy, *R* is the universal constant and *T* represents the absolute temperature. By plotting ln *k* versus 1/T, both the activation energy and the frequency factor can thus be obtained based on the slope and intercept. The calculated E_a for the 2-NP reductive transformation in γ-Al_2O_3 suspensions was 72.5 kJ mol^{-1}, as illustrated in Fig. 3.

3.4. Effects of pH and Fe(II) concentration on Fe(II) adsorption

Fig. 4 shows the effects of pH and the initial Fe(II) concentration on the Fe(II) adsorption in γ-Al_2O_3 suspensions. For a constant initial Fe(II) concentration (e.g., 0.1 mM), an increase in pH resulted in enhanced rates of adsorption. The pH values less than 5.5 corresponded to a negligible Fe(II) adsorption; whereas, the extent of the Fe(II) adsorption reached nearly 90% at pH 7.8. Additionally, the set of experiments at a fixed pH by varying the initial Fe(II) concentration suggested that the fractional adsorption slightly declined with the

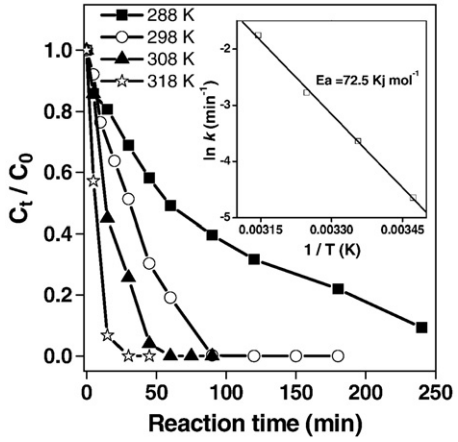

Fig. 3. Effects of temperature on the transformation of 2-NP in γ-Al_2O_3 suspension. The inset shows the plot of ln *k* (the first-order rate constant of 2-NP transformation) against temperature. Reaction conditions: 3 mM $FeSO_4$, 0.022 mM 2-nitrophenol, 0.2 M NaCl, 4.0 g L^{-1} γ-Al_2O_3, pH 6.7, and 288–318 K. C_t = concentration of 2-NP at time *t*; and C_0 = concentration of 2-NP at time zero.

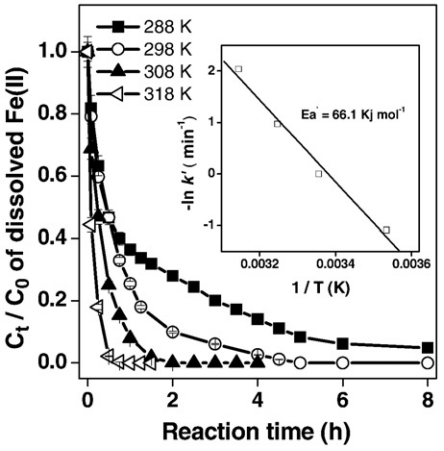

Fig. 5. Effects of temperature on the adsorption of Fe(II) onto γ-Al_2O_3 surfaces. The inset shows the plot of ln *k*′ (the first-order rate constant of Fe(II) adsorption) against temperature. Reaction conditions: 0.1 mM $FeSO_4$, 0.2 M NaCl, 4.0 g L^{-1} γ-Al_2O_3, pH 6.7, and 288–318 K. C_t = concentration of dissolved Fe(II) at time *t*; C_0 = concentration of dissolved Fe(II) at time zero.

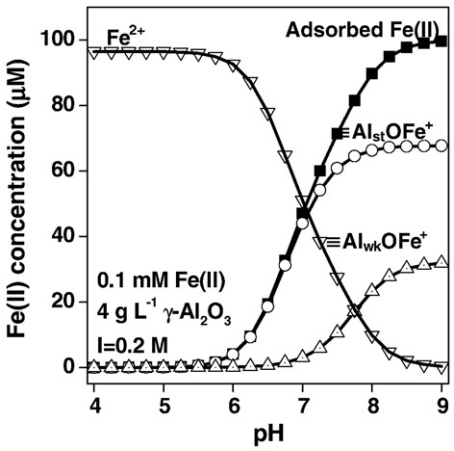

Fig. 6. Calculated distribution of surface complexed Fe(II) species as a function of pH in γ-Al_2O_3 suspensions. The calculation was based on the stability constants provided in Table 1.

increase in the Fe(II) concentration. This trend has commonly been observed for the cation sorption onto hydrous metal oxides (Benjamin and Leckie, 1981; Nano and Strathmann, 2006). The adsorption density (adsorption concentration divided by solid surface area), however, largely increased with the increase of the aqueous Fe(II) concentration. For example, at pH 6.7, the adsorption density was 0.06 μmol m^{-2} in response to an initial Fe(II) concentration of 0.1 mM; it rose to 0.15 μmol m^{-2} when associated with an initial Fe(II) concentration of 0.5 mM.

3.5. Effects of temperature on the Fe(II) adsorption

Fig. 5 reveals the dependence of the Fe(II) adsorption on temperature in γ-Al_2O_3 suspensions. At a fixed temperature, a rapid adsorption of Fe(II) within minutes was followed by much slower adsorption. This was consistent with the other reports concerning the influence of temperature on metal ion adsorption (Coughlin and Stone, 1995; Pecher et al., 2002; Nano and Strathmann, 2006). A careful evaluation of the adsorbed Fe(II) concentration as a function of time demonstrated that the adsorption at constant temperature follows the first-order kinetic law. It was also found that the first-order kinetic constant (k') of Fe(II) adsorption increased with the increase of temperature. Calculation results showed that the k' values of the Fe(II) adsorption onto γ-Al_2O_3 at 318 K was nearly 20 times larger than that at 288 K. The resulting temperature-dependent adsorption is likely due to the breaking of some internal bonds near the edge of the particles with the increased temperature; the breaking of bonds in turn allows an increased adsorption of the surface-bound Fe(II) species (Mohan and Chander, 2006). A plot of ln k' against 1/T can yield E_a according to the Arrhenius Eq. (2) (Fig. 5). The activation energy of Fe(II) adsorption onto γ-Al_2O_3 was 66.1 kJ mol^{-1}, suggesting the adsorption under this condition was a chemically controlled process (Liu and Huang, 2003).

To summarize all the results obtained from the adsorption and kinetic study, it can be concluded that an increase in pH, Fe (II) concentration or reaction temperature gives rise to an elevated density of the Fe(II) ions adsorbed to mineral surfaces, which further results in an enhanced reaction rate of 2-NP reduction.

3.6. Surface complexation modeling

It has been reported that Fe(II) adsorption onto γ-Al_2O_3 surfaces can be well described by the diffuse double layer (DDL) surface complexation model (Nano and Strathmann, 2006), which considers the formation of $\equiv SOFe^+$ complexes at both weak-binding and strong-binding sites. The distribution of surface complexed Fe(II) species in γ-Al_2O_3 suspensions was then investigated by the use of stability constants listed in Table 1. Fig. 6 shows the distinct difference in the extent of each individual species in terms of various pH values. For pH<7, only the $\equiv Al_{st}OFe^+$ species (strong-binding surface complex) was present. An increase in pH led to the formation of $\equiv Al_{wk}OFe^+$ species (weak-binding surface complex) and the increase in concentrations of both $\equiv Al_{st}OFe^+$ and $\equiv Al_{wk}OFe^+$ species. For pH>8.5, both of them arrived at relatively constant values, leveling off at 70% and 30%, respectively. Obviously, in our case (the investigated pH is less than 7.5), the dominant Fe(II) surface complex in γ-Al_2O_3 suspensions was $\equiv Al_{st}OFe^+$ whose density was the only factor to determine the reductive transformation of the 2-NP in the scope of this study.

3.7. Effects of surface complexation speciation on k values

As demonstrated above, pH is a crucial factor to influence the density of adsorbed Fe(II) as well as the surface complexation speciation onto γ-Al_2O_3 surfaces; likewise, pH plays a significant role in determining the k value of 2-NP reduction in heterogeneous systems. It is thus important to establish the relationship between the densities of different surface complexation species and k values under different pH control. Fig. 7 shows the scatter plots of measured k values against the concentrations of $\equiv Al_{st}OFe^+$ and $\equiv Al_{wk}OFe^+$. In general, scatter plots with R^2 values that approach unity indicate significant linear correlations. It was found that the k values for the 2-NP reduction

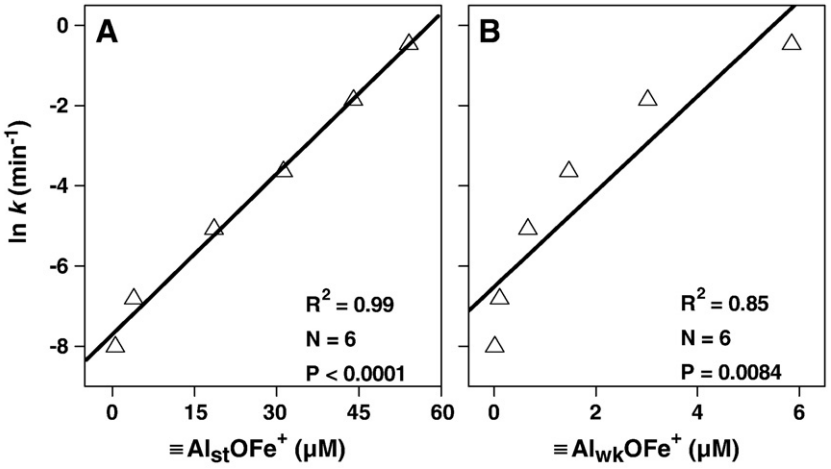

Fig. 7. Correlation scatter plots for the k values of 2-NP transformation versus different surface complexed Fe(II) species in γ-Al_2O_3 suspensions.

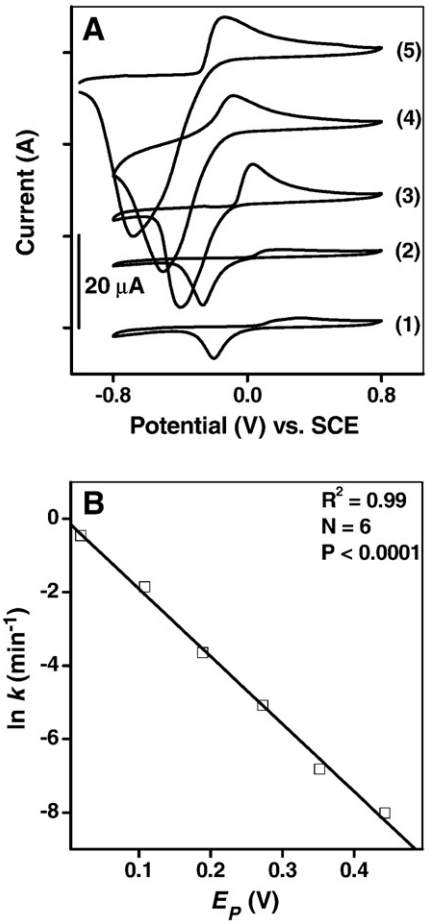

Fig. 8. (A) Cyclic voltammograms of Fe(II) adsorbed onto γ-Al_2O_3 electrodes. Electrochemical measurements were conducted in the 25 mL cell containing 3.0 mM $FeSO_4$, 0.2 M NaCl solution and 28 mM buffer at different pH values on the γ-Al_2O_3-modified glassy carbon (GC) electrodes at 298 K . Scan rate was 50 mV s^{-1}. (1) pH = 5.5; (2) pH = 6.0; (3) pH = 6.5; (4) pH = 7.0; and (5) pH = 7.5. (B) Dependence of ln *k* on the Fe(II) oxidation peak potential obtained from CV tests.

exhibited a very strong correlation with the concentration of the $\equiv Al_{st}OFe^{+}$ complex ($R^2 = 0.99$). On the other hand, the R^2 value was only 0.85 with respect to the $\equiv Al_{wk}OFe^{+}$ complex. These results further demonstrated the $\equiv Al_{st}OFe^{+}$ complex was the key species influencing the *k* value.

3.8. Electrochemical evidence of the change in Fe^{III}/Fe^{II} redox potential

Voltammograms of adsorbed Fe(II) species on the γ-Al_2O_3-modified GC electrode at various pH values provide a direct evidence of the change in its redox behavior. It should be noted that repeatable scans of CV were performed, and that there was insignificant difference in the peak position with respect to the first three cycles, demonstrating the stability of the coated electrode (data not shown). Fig. 8A shows the results relative to the first cycle. All CVs exhibited a pair of peaks: an anodic oxidation peak for Fe(II) at potentials ranging from −0.2 V to 0.4 V (versus SCE) and a cathodic reduction peak for Fe (III) at potentials ranging from −0.6 V to −0.2 V (versus SCE). Clearly visible was the negative shift of the peak oxidation potential (denoted as E_p) of Fe(II) as a function of solution pH.

It was predicted from the SCM modeling (data not shown) that the distribution of Fe(II) speciation was linearly dependent on the mineral loading in the range from 0.0004 g/L to 4.0 g/L. Although the loading of mineral (estimated to be 0.002 g/L) in the electrochemical system is much lower compared to that used in both kinetic and adsorption studies, it seems reasonable to correlate CV data with the kinetic and adsorption data presented above. The combination of Figs. 8A and 6 suggested that at low pH (e.g., pH 5.5), the aqueous Fe(II) in the solution could play a significant role in determining E_p. In contrast, at relatively high pH (e.g., pH 7.0), the dominant surface species ($\equiv Al_{st}OFe^{+}$) could contribute to a more negative oxidation potential. In general, the negative shift of the Fe(II) oxidation potential thermodynamically reflects the movement of the Gibbs free-energy to a negative value. Also, the previous reports (Strathmann and Stone, 2002a,b) have demonstrated that the Gibbs free-energy change had a pronounced effect on the reaction kinetics of reductive transformation of an organic pollutant, according to the linear free-energy relationship (LFER). Accordingly, Fig. 8B presents the relationship between ln *k* of the 2-NP transformation and E_p (versus SHE). A good linear correlation was found, as indicated by the high R^2 value (0.99). It thus can be concluded that an increase in the concentration of the $\equiv Al_{st}OFe^{+}$ surface complex might result in a negative shift of Fe(II) oxidation potential, which accounts for the enhanced transformation rates of the 2-NP.

4. Conclusion

We have successfully demonstrated that the 2-NP can be effectively reduced in the presence of γ-Al_2O_3-bound Fe(II) species. The first-order rate constant (*k* value) was found to be highly dependent on the variation in experimental parameters including pH, Fe(II) concentration, and temperature. The resulting enhanced reaction rates were contributed to the increase in the adsorption concentration of the surface complexed Fe(II). By use of a two-site model to calculate the concentration of individual Fe(II) species, it has been revealed that the dominant Fe(II) surface complex in γ-Al_2O_3 suspension was $\equiv Al_{st}OFe^{+}$. Moreover, CV tests provided direct evidence of negative shift of the peak oxidation potential of Fe(II) resulted from the increased concentration of $\equiv Al_{st}OFe^{+}$ with the increase of pH. A good linear relationship between ln *k* and the Fe(II) peak oxidation potential was observed. These findings have implications for our general understanding of Fe(II) redox reactivity in more complicated heterogeneous anoxic environments.

Acknowledgement

The work was financially supported by the National Natural Science Foundation of PR China (No. 20577007, 40771105).

References

Benjamin, M.M., Leckie, J.O., 1981. Multiple-site adsorption of Cd, Cu, Zn, and Pb on amorphous iron oxyhydroxide. J. Collid Interface Sci. 79 (2), 209–221.
Buerge, I.J., Hug, S.J., 1998. Influence of organic ligands on chromium (VI) reduction by iron(II). Environ. Sci. Technol. 32 (14), 2092–2099.
Colon, D., Weber, E.J., Anderson, J.L., Winget, P., Suarez, L.A., 2006. Reduction of nitrosobenzenes and *N*-Hydroxylanilines by Fe(II) species: elucidation of the reaction mechanism. Environ. Sci. Technol. 40 (14), 4449–4454.
Coughlin, B.R., Stone, A.T., 1995. Nonreversible adsorption of divalent metal ions (Mn^{II}, Co^{II}, Ni^{II}, Cu^{II}, and Pb^{II}) onto goethite: effects of acidification, Fe^{II} addition, and picolinic acid addition. Environ. Sci. Technol. 29 (9), 2445–2455.
Fadrus, H., Malý, J., 1975. Rapid extraction-photometric determination of traces of iron (II) and iron(III) in water with 1,10-phenanthroline. J. Anal. Chim. Acta. 77, 315–316.
Frank, M.D., Rene, P.S., Donald, L.M., 1992. Reduction of substituted nitrobenzenes in aqueous solutions containing natural organic matter. Environ. Sci. Technol. 26 (11), 2133–2141.
Hiemstra, T., Riemsdijk, W.H., 2007. Adsorption and surface oxidation of Fe(II) on metal (hydr)oxides. Geochim. Cosmochim. Acta. 71 (24), 5913–5933.
Hofstetter, T.B., Heijman, C.G., Haderlein, S.B., Holliger, C., Schwarzenbach, R.P., 1999. Complete reduction of TNT and other (Poly)nitroaromatic compounds under iron-reducing subsurface conditions. Environ. Sci. Technol. 33 (9), 1479–1487.
Jeon, B.H., Dempsey, B.A., Burgos, W.D., Barnett, M.O., Roden, E.E., 2005. Chemical reduction of U(VI) by Fe(II) at the solid-water interface using natural and synthetic Fe(III) oxides. Environ. Sci. Technol. 39 (15), 5642–5649.
Klausen, J., Trober, S.P., Haderlein, S.B., Schwarzenbach, R.P., 1995. Reduction of substituted nitrobenzenes by Fe(II) in aqueous mineral suspensions. Environ. Sci. Technol. 29 (9), 2396–2404.

Klupinski, T.P., Chin, Y.P., Traina, S.J., 2004. Abiotic degradation of pentachloronitrobenzene by Fe(II): reactions on goethite and iron oxide nanoparticles. Environ. Sci. Technol. 38 (16), 4353–4360.

Li, F.B., Wang, X.G., Li, Y.T., Liu, C.S., Zeng, F., Zhang, L.J., Hao, M.D., Ruan, H.D., 2008. Enhancement of the reductive transformation of pentachlorophenol by polycarboxylic acids at the iron oxide-water interface. J. Collid Interface Sci. 321 (2), 332–341.

Liu, C., Huang, P.M., 2003. Kinetics of lead adsorption by iron oxides formed under the influence of citrate. Geochim. Cosmochim. Acta. 67 (5), 1045–1054.

Martell, A.E., Smith, R.M., Motekaitis, R.J., 1997. Critically selected stability constants of metal complexes database. Version 4.0, U.S. Department of Commerce, National Institute of Standards and Technology, Gaithersbug, MD.

Maithreepala, R.A., Doong, R.A., 2004. Synergistic effect of copper ion on the reductive dechlorination of carbon tetrachloride by surface-bound Fe(II) associated with goethite. Environ. Sci. Technol. 38 (1), 260–268.

Mohan, D., Chander, S., 2006. Single, binary, and multicomponent sorption of iron and manganese on lignite. J. Collid Interface Sci. 299 (1), 76–87.

Naka, D., Kim, D., Strathmann, T.J., 2006. Abiotic reduction of nitroaromatic compounds by aqueous iron(II)-catechol complexes. Environ. Sci. Technol. 40 (9), 3006–3012.

Nano, G.V., Strathmann, T.J., 2006. Ferrous iron sorption by hydrous metal oxides. J. Collid Interface Sci. 297 (2), 443–454.

Nano, G.V., Strathmann, T.J., 2008. Application of surface complexation modeling to the reactivity of iron(II) with nitroaromatic and oxime carbamate contaminants in aqueous TiO_2 suspensions. J. Collid Interface Sci. 321 (2), 350–359.

Pecher, K., Haderlein, S.B., Schwarzenbach, R.P., 2002. Reduction of polyhalogenated methanes by surface-bound Fe(II) in aqueous suspensions of iron oxides. Environ. Sci. Technol. 36 (8), 1734–1741.

Rene, P.S., Ruth, S., Klaus, L., Josef, Z., 1990. Quinone and iron porphyrin mediated reduction of nitroaromatic compounds in homogeneous aqueous solution. Environ. Sci. Technol. 24 (10), 1566–1574.

Rugge, K., Hofstetter, T.B., Haderlein, S.B., Bjerg, P.L., Knudsen, S., Zraunig, C., Mosbaek, H., Christensen, T.H., 1998. Characterization of predominant reductants in an anaerobic leachate-contaminated aquifer by nitroaromatic probe compounds. Environ. Sci. Technol. 32 (1), 23–31.

Rush, J.D., Koppenol, W.H., 1987. The reaction between ferrous polyaminocarboxylate complexes and hydrogen peroxide: an investigation of the reaction intermediates by stopped flow spectrophotometry. J. Inorg. Biochem. 29 (3), 199–215.

Schoonen, M.A.A., Xu, Y., Strongin, D.R., 1998. An introduction to geocatalysis. J. Geochem. Exploration. 62 (1), 201–215.

Strathmann, T.J., Stone, A.T., 2002a. Reduction of the pesticides oxamyl and methomyl by Fe^{II}: effect of pH and inorganic ligands. Environ. Sci. Technol. 36 (4), 653–661.

Strathmann, T.J., Stone, A.T., 2002b. Reduction of oxamyl and related pesticides by Fe^{II}: influence of organic ligands and natural organic matter. Environ. Sci. Technol. 36 (23), 5172–5183.

Strathmann, T.J., Stone, A.T., 2003. Mineral surface catalysis of reactions between Fe^{II} and oxime carbamate pesticides. Geochim. Cosmochim. Acta. 67 (15), 2775–2791.

Stumm, W., Sulzberger, B., 1992. The cycling of iron in natural environments—considerations based on laboratory studies of heterogeneous redox processes. Geochim. Cosmochim. Acta. 56 (8), 3233–3257.

Torrents, A., Ph.D. Thesis, Department of Geography and Environmental Engineering, The Johns Hopkins University, Baltimore, MD. 1992.

Yan, L.B., Bailey, G.W., 2001. Sorption and abiotic redox transformation of nitrobenzene at the smectite-water interface. J. Colloid Interface Sci. 241 (1), 142–153.